Dynamics and Rheology of Supramolecular Assemblies at Elevated Pressures

Nikolaos Burger, Gerhard Meier, Laurent Bouteiller, Benoit Loppinet, Dimitris Vlassopoulos

Dynamics and Rheology of Supramolecular Assemblies at Elevated Pressures

Nikolaos A. Burger[1,2], Gerhard Meier[3],

Laurent Bouteiller[4], Benoit Loppinet[1], Dimitris Vlassopoulos[1,2 *]

1 Foundation for Research & Technology Hellas (FORTH), Institute for Electronic Structure & Laser, Heraklion 70013, Greece

2 University of Crete, Department of Materials Science & Technology, Heraklion 70013, Greece

3 Forschungszentrum Jülich, Biomacromolecular Systems and Processes (IBI-4), 52425 Jülich, Germany

4 Sorbonne Université, CNRS, IPCM, Equipe Chimie des Polymères, 75005 Paris, France

Email: dvlasso@iesl.forth.gr (D. Vlassopoulos)

Abstract

A methodology to investigate the linear viscoelastic properties of complex fluids at elevated pressures (up to 120 MPa) is presented. It is based on a dynamic light scattering (DLS) setup coupled with a stainless steel chamber, where the test sample is pressurized by means of an inert gas. The viscoelastic spectra are extracted through passive microrheology. We discuss an application to a hydrogen bonding motif 2,4-bis(2-ethylhexylureido)toluene (EHUT), which self-assembles into supramolecular structures (tubes and filaments) in apolar solvents, dodecane and cyclohexane. High levels of pressure (roughly above 20 MPa) are found to slow-down the terminal relaxation process, however the increase in the entanglement plateau modulus and the associated persistence length is not significant. The concentration dependence of the plateau modulus, relaxation times (fast and slow) and correlation length is practically the same for all pressures and exhibits distinct power-law behavior in different regimes. Within the tube phase in dodecane, the relative viscosity increment is weakly enhanced with increasing pressure and reaches a plateau at about 60 MPa. In fact, depending on concentration, the application of pressure in the tube regime may lead to a transition from viscous (unentangled) to viscoelastic (partially-entangled to well-entangled

state) solution. For well entangled, long tubes, the extent of the plateau regime (ratio of high- to low-moduli crossover frequencies) increases with pressure. The collective information from these observations is summarized in a temperature-pressure state diagram. These findings provide ingredients for formulation of a solid theoretical framework to better understand and exploit the role of pressure on the structure and dynamics of supramolecular polymers.

I. INTRODUCTION

Pressure is often considered as the "forgotten thermodynamic variable", in part because precise experiments at high pressures are challenging, however its impact can be significant and has been widely considered in various situations in science and technology.[1-4] It may induce microstructural changes in soft materials with consequences on their phase behavior and, especially, dynamics. Typical examples include, but are not limited to polymer melts and solutions, glass forming liquids, colloidal dispersions, self-assemblies, biomaterials and other technologically relevant materials like bitumen.[5-14] Focusing on rheology, a substantial increase in the viscosity of branched polyethylenes with increasing pressure was already reported in the late 50s.[15] Extensive studies, primarily with capillary rheology and polyolefins, have revealed the role of pressure on increasing viscosity and reducing wall slip velocity.[16-18] The use of rotational instruments offers the advantage of giving access to the entire linear viscoelastic (LVE) spectrum as well as nonlinear viscometric material functions, but is limited to relatively low pressures (typically not exceeding 20 MPa, although some commercial rheometer vendors offer options claimed to reach 100 MPa, mostly with liquids).[2,4,19] Recently, the pressure-dependent viscosity (up to 100 MPa) in hydrogels of host-guest type was investigated with a Couette geometry in a commercial device.[20] It was found that pressure did interfere with the association-dissociation process but did not affect their viscosity. Hence, pressure is an important variable that may affect supramolecular associations and their properties, and exploring and exploiting its role represents the motivation for the present work.

An alternative approach to high-pressure rheometry is taking advantage of passive microrheology. This is based on the (often assumed) validity of the generalized Stokes-Einstein relation (GSER), which links the mean squared displacement (MSD) of a tracer (probe) particle to the stress relaxation modulus of the investigated sample (see Figure 4 and detailed description below). The particle is chosen such that is does not adsorb on the test sample (here, supramolecular polymer) and does sense its fluctuations (having a size larger than that of the test material). Typically, the MSD is measured by dynamic light scattering

(DLS) techniques.[14, 21-24] Different specialized sample cells for handling elevated pressures have been developed and utilized in neutron or X-ray scattering facilities or in conjunction with static or dynamic light scattering setups.[14, 25-29] DLS-based microrheological LVE data were reported in the past[30] and very recently, a comprehensive study reported the design and implementation of a versatile experimental setup to obtain reliable data with fracturing fluids at pressures up to 200 MPa.[23] Both investigations used passive microrheology based on diffusive wave spectroscopy (DWS).

In this work we present a methodology to measure the high-pressure linear viscoelasticity (HP-LVE) of a supramolecular polymer in apolar solvents (n-dodecane and cyclohexane) by means of passive DLS-microrheology in the single scattering limit. This limit can be reached if the refractive index contrast of the examined solution is low and scattering is mainly due to the added tracer particles (at very low fraction), as reported for similar systems[14,30] and for DNA-star solutions and gels.[31] However, passive microrheology in this limit has not been explored at high pressures; therefore, we focus here on probing the dynamic structure (intermediate scattering function) of supramolecular polymer solutions at high pressures and extracting their LVE properties.

When bisurea-based molecules 2,4-bis(2-ethylhexylureido)toluene (EHUT) are added to apolar solvents, depending on temperature and concentration they self-assemble into two distinct supramolecular structures (tubes and filaments) by means of hydrogen bonding.[32-34] Figure 1 (top) illustrates schematically the complete dynamic phase diagram of EHUT in alkanes. Depending on the choice of solvent, there are quantitative but not qualitative differences, hence this diagram is rather generic. In solvents whose molecular structure consists of long linear backbones (such as decane and dodecane), the tube-to-filament transition takes place at high temperatures. On the other hand, in solvents bearing aromatic groups (for example, cyclohexane or toluene) the transition temperature drops substantially. Solutions of these supramolecular assemblies exhibit remarkable rheological properties. In the tube (long and thick assemblies with three molecules comprising the cross-section) phase they vary from low-viscosity liquids to highly viscoelastic liquids or gels, whereas filaments (short and thin assemblies with one molecule in the cross section) form low-viscosity liquids.[35-37]

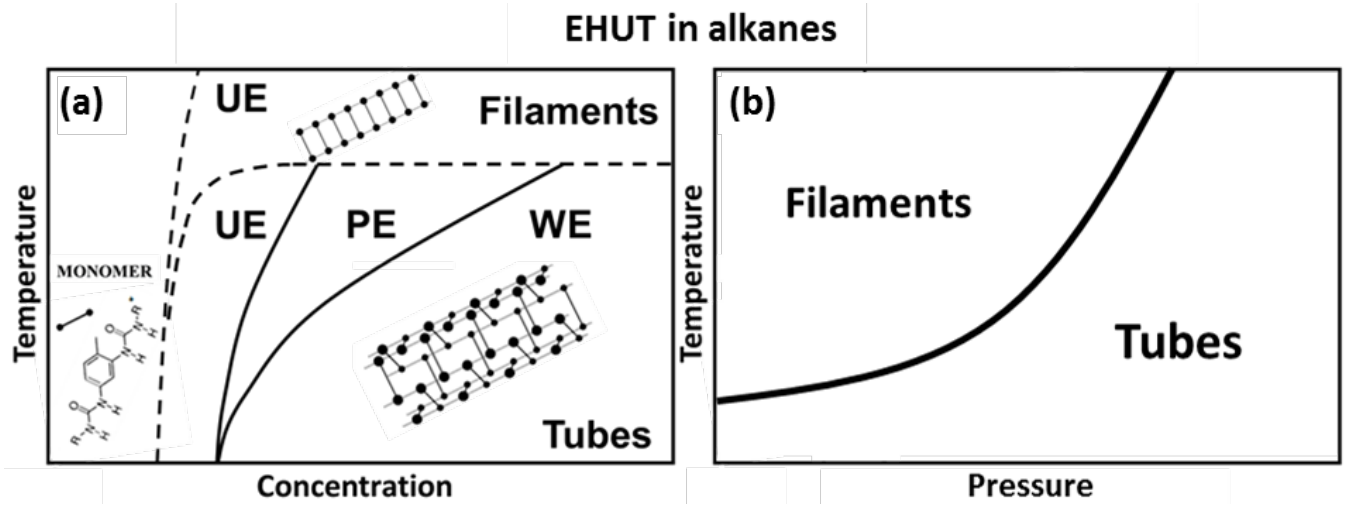

Figure 1: (a) Schematic of a complete dynamic phase diagram of EHUT molecules in alkanes. The two dashed lines indicate the boarders separating different structures (phases): free monomers (at low concentrations), Tubes (higher concentrations low temperatures) and Filaments (high temperatures and concentrations). Black lines separate the unentangled (UE), partially entangled (PE) and well entangled (WE) assemblies, respectively. (b) Schematic phase diagram in the temperature-pressure space for a specific concentration of EHUT/ cyclohexane solution. Inspired from Ref.14.

Application of pressure was recently shown to induce structural transition in these supramolecular assemblies, and in particular to stabilize the tube phase.[14] A schematic illustration of the temperature-pressure phase diagram at a concentration corresponding to the tube phase at ambient conditions is shown in Figure 1(b).

These hydrogen-bonding assemblies were recently reported to be very sensitive to traces of water, as revealed by rheological measurements at different levels of relative humidity.[38] Although the phenomenon appears to be universal for hydrogen-bonded assemblies in organic solvents[39], the exact mechanism remains a subject of debate. One school of thought suggests that water molecules enter the supramolecular chains and effectively copolymerize with them[39] and another calls for water causing scission of the chains via a chain stopper effect.[38,40-44] The linear viscoelastic properties of supramolecular polymers (also called living polymers) forming entanglements akin to those of conventional polymers, can be quantified in the framework of the classic model of Cates:[45-49] there are two characteristic relaxation times, the local breaking time (τ_b) due to the exchange of associating units (lifetime of bonds), and the terminal relaxation time (τ_t) of the entire assembly, $\tau_t = (\tau_{rep}\, \tau_b)^{1/2}$, where τ_{rep} is the reptation time of the living assembly (this expression holds in the limit $\tau_b << \tau_{rep}$). The model predicts that $\tau_t \sim c^{1.25}$ and $G_0 \sim c^{2.25}$.[50] In the absence of humidity, the scaling for the modulus was confirmed, but not that for the terminal relaxation time

(where a lower exponent, by about half, was reported).[38] Recently, Larson and co-workers combined rheology, scattering and simulations and provided quantitative estimates for the characteristic lengths of supramolecular polymer solutions.[51-53] These assemblies are characterized by a length distribution which affects the rheological properties.[49] Using efficient chain stoppers or increasing temperature we can induce changes of their length (which in general follows Arrhenius behavior, $< L > \sim e^{(\frac{E}{k_B T})}$, where E is the activation energy associated with bonding, k_B the Boltzmann constant and T the absolute temperature).[40-44] In this study we report that pressure can also induce changes of the average length, <L> as illustrated schematically in Figure 2.

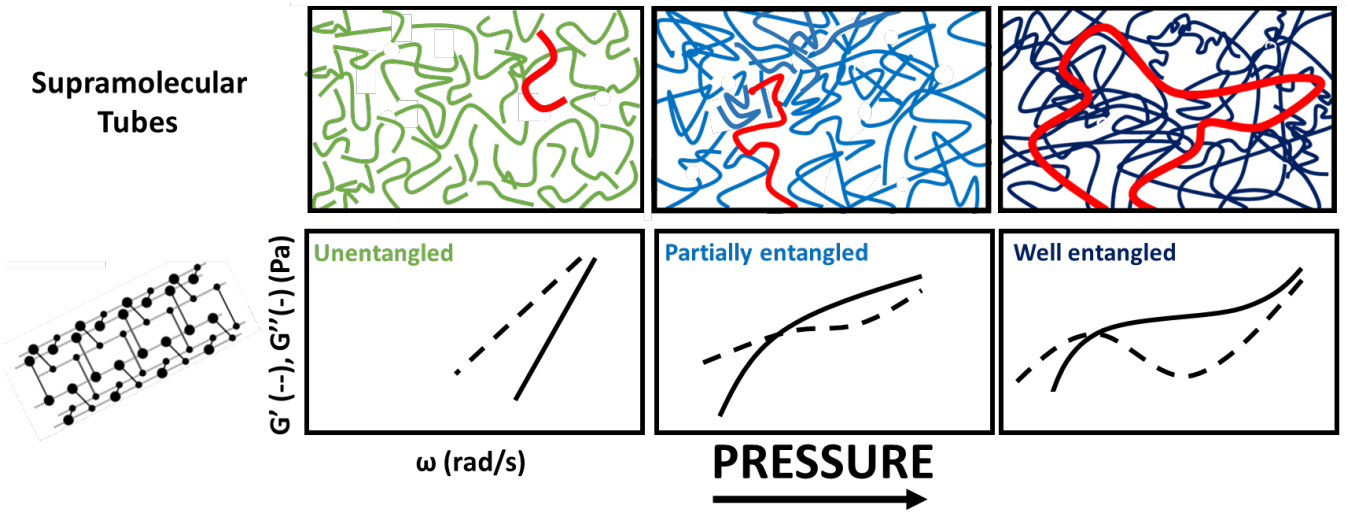

Figure 2: Schematic illustration of a non-dilute solution of a supramolecular assembly forming tubes, with the network structure and its viscoelastic signature changing from unentangled to partially entangled to well entangled as the pressure increases.

Given the above developments, exploring the role of elevated pressure to reversible supramolecular assemblies which exhibit different conformation, phase and dynamics in the temperature – concentration space, emerges as a formidable challenge. We address this challenge in this work and we focus in particular on the phase behavior and linear viscoelasticity of EHUT solutions in two apolar solvents, n-dodecane and cyclohexane, where we expect that elevated pressures will play a role on their dynamics by affecting the hydrogen bonding interactions. We first describe the high-pressure DLS setup for passive microrheology and then present and critically discuss the results obtained with the two different solutions

over a range of concentrations temperatures and pressures, under originally ambient humidity conditions (however, reference to the effects of reduced humidity will be made as needed).

EXPERIMENTAL

MATERIALS

EHUT was obtained by reacting racemic 2-ethylhexylamine with 2,4-toluene diisocyanate.[36] Two apolar solvents were used as received from Sigma Aldrich, dodecane (99+ % pure) and cyclohexane (99.7 % pure). Both have nearly the same dielectric constant (2.01 and 2.02, respectively, much smaller than that of water, 78.5).[54] The solutions were prepared at ambient relative humidity (about 40%) and temperature of 80ºC for dodecane and about 25ºC for cyclohexane, by adding EHUT powder to the solvent and stirring for at least 48 hours. For the microrheological experiments, polymethylmethacrylate (PMMA) particles were added at a volume fraction of about 10^{-4}, to act as probes. The particles, chemically grafted with poly(hydroxystearic acid) (PHSA) chains (with a length of about 10nm) to ensure proper dispersion, have a total hydrodynamic radius R_h=130 nm (with a polydispersity in the order of 10%).[55] This length scale is much higher than the characteristic length of the supramolecular network[14] and ensures reliable microrheological measurements of its LVE properties.[56] At 25ºC the PMMA probes have a refractive index value 1.49 and the solvents 1.42.

METHODS

High-Pressure DLS

Figure 3 shows a schematic illustration of the homemade high-pressure cell made for the DLS experiments. A cw Nd-Yag laser at 532nm was used and the glass windows enabled measuring at three different scattering angles at θ= 45, 90 and 135^0. In this study measurements were performed at 90^0 only. A mono-mode optical fiber was used to transfer the scattered light into a photomultiplier tube (PMT). The solution was pressurized by means of nitrogen gas, as shown in the figure. The diffusion of nitrogen inside the material is too slow to be a concern, i.e., the nitrogen molecules (which are introduced on top of the free surface of the investigated solution in the cell) do not reach the DLS probe volume during the measurement.[14, 57] In fact, experiments were performed at relatively short times (order of hours), compared to the diffusion time of nitrogen molecules which is of the order of days. Reproducibility tests at different

pressure cycles and for long period of times confirmed the accuracy of the measurements and stability of the samples (see Figure S1 of the Supporting Information).

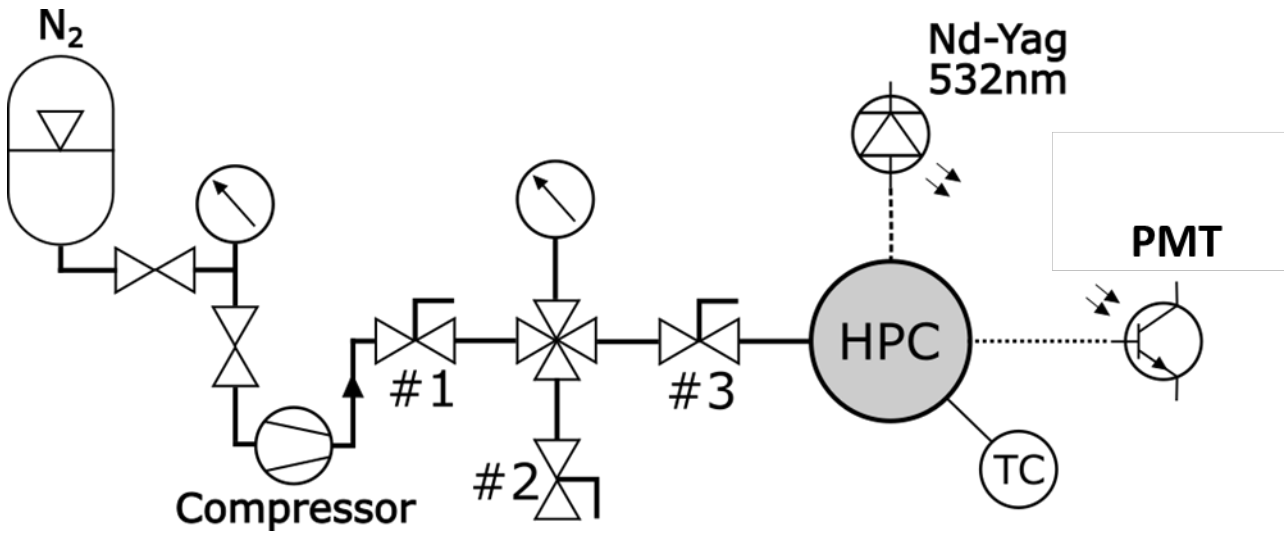

Figure 3: Schematic illustration of the experimental high-pressure DLS setup. The different fixtures are shown (out of scale) from left: nitrogen gas (N_2) cylinder, pressure regulator with manometer (with left-pointing arrow), membrane compressor, hand-operated valves (#1,2,3) to control the direction /flow rate of nitrogen into the high pressure cell (HPC) with glass windows (at fixed scattering angles of 45, 90 and 135°), temperature controller (TC), Nd-Yag laser at 532 nm, with a power of about 80 mW, and a photomultiplier tube (PMT) that receives the scattered light for subsequent signal analysis.

The electric field auto-correlation function (or intermediate scattering function) of the light reaching the detector at time *t* after a lag time τ_w, $g_1(\tau_w, t)$, is given by

$$g_1(\tau_w, t) = \frac{<E(\tau_w+t)E^*(\tau_w)>}{<|E(\tau_w+t)|^2>} \quad (1)$$

where *E* is the electric field at the detector and *E** its complex conjugate. Typically, a photodetector measures the light intensity, $I=E^*E$ for homodyne conditions. The normalized intensity auto-correlation function originates from the fluctuations of the scattering intensity of the medium over time and is given by the following equation:

$$g_2(\tau_w, t) = \frac{<I(\tau_w+t)I(\tau_w)>}{<|I(\tau_w+t)|^2>} \quad (2)$$

For an ergodic medium, where ensemble and time averages are equal, g_1 and g_2 are related via the Siegert relation,

$$g_2(t) = 1 + \beta \, |g_1(t)|^2 \qquad (3)$$

where β is an experimental constant accounting for the short-time intercept (dynamical contrast) of the correlation function. Hence, by measuring the intensity correlation function we are able to derive the field correlation (intermediate scattering) function $C(t) = g_1(t)$.

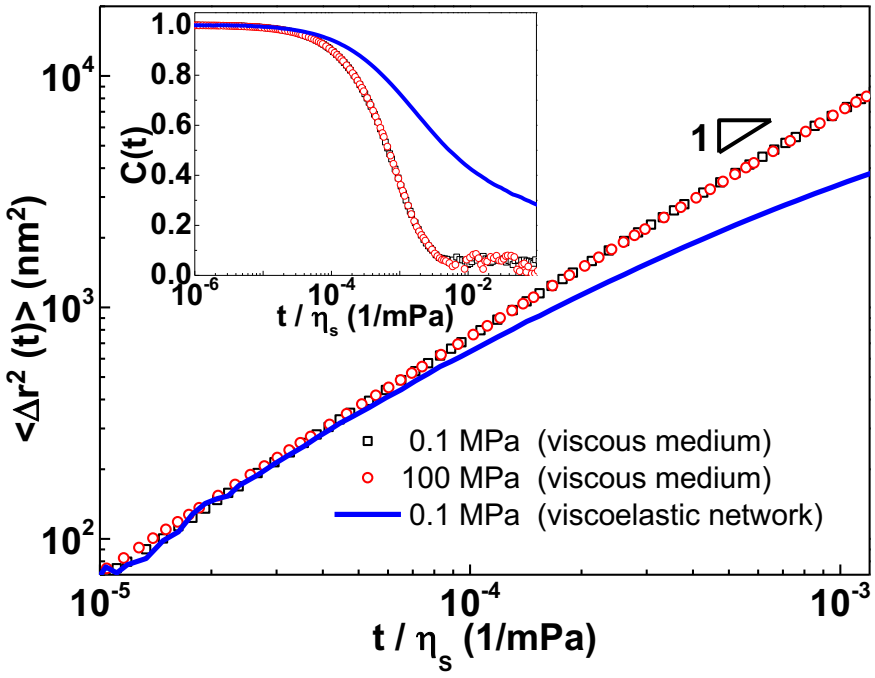

Figure 4: Mean square displacement, extracted from the field correlation function C(t) (inset), of pure dodecane (with added PMMA probes, see text) at 25 °C and two different pressures (open black squares for 0.1 MPa and open red circles for 100 MPa). For comparison, respective data of an EHUT tube viscoelastic network at 0.1 MPa are also shown (solid line). The time (horizontal axis) is scaled with the solvent viscosity, η_s, taken from Ref.58. Pressure-dependent viscosity data of dodecane solvent are depicted in Figure S2.

In case the scattered intensity arises from dilute colloidal tracers, the electric field autocorrelation function $g_1(t)$ is related to the mean square displacement $\langle \Delta r^2 \rangle$ of the colloidal probe particle by

$$g_1(\tau, q) = g_1(0)\exp\left(\frac{-q^2\langle\Delta r^2(\tau)\rangle}{6}\right) \quad (4)$$

where the scattering wave vector (q) is a function of the refractive index (n), the wavelength of laser light (λ) and the scattering angle (θ)

$$q = \frac{4\pi n}{\lambda}\sin\left(\frac{\theta}{2}\right) \quad (5)$$

For a viscous fluid, the Stokes-Einstein-Sutherland equation (6) below links the macroscopic (viscosity) and microscopic (thermal energy k_BT) properties. Here, the hydrodynamic radius of the embedded particle is R_h=130 nm, which yields $qR_h \approx 3$; this value corroborates the notion that we probe the self-diffusion of the particle in the present non-dilute, yet not highly concentrated EHUT solutions. Furthermore, in a medium of viscosity η_s, the diffusion coefficient of the embedded probe is

$$D = \frac{k_BT}{6\pi\eta_s R_h} \quad (6)$$

The respective probe motion is characterized by its Mean Square Displacement (MSD) $\langle\Delta r^2\rangle$ as a function of time

$$\langle\Delta r^2(\tau)\rangle = 6\,Dt \quad (7)$$

For a viscoelastic medium (see Figure 4), the GSER can be written as

$$\langle\Delta r^2\rangle(t) = \frac{k_BT}{\pi R_h}J(t) \quad (8)$$

where $J(t)$ is the creep compliance.[56,60] $J(t)$ is then transformed into the frequency-dependent shear moduli $G'(\omega), G''(\omega)$ using a nonlinear regularization procedure (NLREG) which is based on Tikhonov regularization, as described in the literature.[60] Passive microrheology, which deduces shear moduli from measured thermal motion of probe particles in a complex fluid, is discussed extensively in the literature.[56,59,60]

For PMMA particles dispersed in a molecular solvent (dodecane), the intermediate scattering functions at 0.1 MPa and 100 MPa are well-fitted with a single exponential for purely diffusive motion, and this is also reflected in the mean square displacements which exhibit of long-time dependence with a power-law of 1 (Figure 4), yielding the diffusion coefficient. In addition, this figure corroborates the fact that the hydrodynamic radius of the PMMA probes used in this study does not change significantly in the studied pressure range. If, on the other hand, the tracers are added to an EHUT viscoelastic tube network, the situation is more complicated and characterized by a clear departure from the single exponential purely diffusive behavior. This will be further discussed below.

Figure 5 confirms the robustness of the implemented DLS-microrheological approach in the single scattering limit. The microrheological LVE spectra compare very well with the respective bulk rheological data at low frequencies (LF) and intermediate frequencies (gray regime in the figure), in harmony with earlier findings on wormlike surfactant micelles.[63] The LF regime is the terminal flow (with G'~ ω and G''~ ω^2) as described by the model of Cates. In the intermediate regime there is good agreement between the two methods, and the small deviation of the microrheology data is likely due to the process to extract the LVE data from the MSD (see above). In this spirit, the apparent higher G' plateau regime on approaching the high frequency (HF) regime (roughly in the range 300-3000 rad/s) will not be considered further (however, the HF G''-slope of 0.75 will be discussed below). Moving to the HF regime, one should be careful in interpreting the data from microrheology because the validity of the GSER may be questionable. If the measured scattering intensity is due to the self-diffusion of the probe, then the conversion from the MSD to the frequency-dependent moduli should be accurate enough to allow for a reasonable estimation of the persistence length.[14]

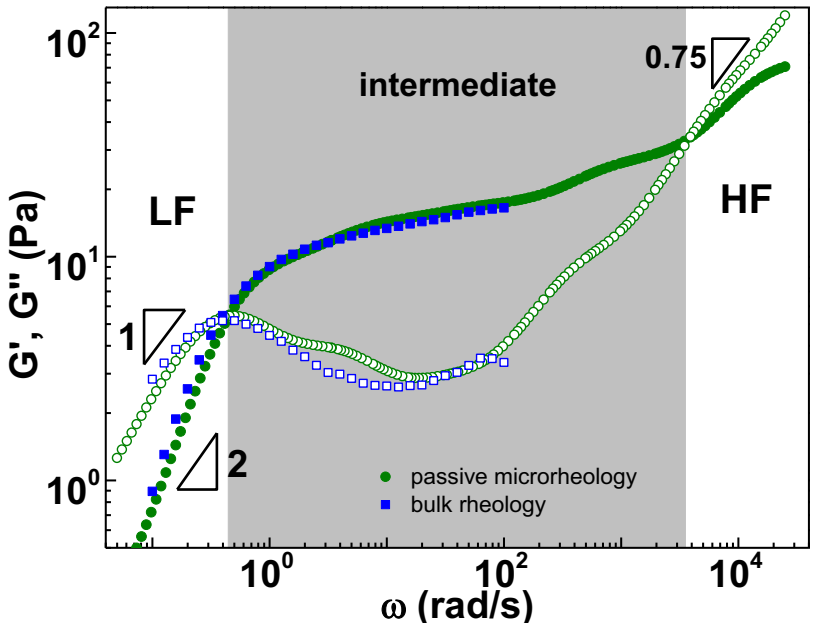

Figure 5. Linear viscoelastic spectra (filled symbols for G', open for G'') of EHUT/dodecane solutions at c=3.6 g/L, T=25°C and 0.1 MPa, obtained from microrheology (green circles) and conventional rheology (blue squares). The intermediate frequency regime between the high-frequency (HF) and low-frequency (LF) moduli crossovers is gray-shaded. The terminal slopes (1,2) and HF slope (0.75) are also indicated.

EHUT assemblies in apolar solvents: Same structure (tubes), different LVE

To appreciate the significance of the choice of solvent, we show in Figure 6 the LVE spectra at 0.1 MPa and 25°C for two different EHUT solutions of similar concentrations, dissolved in the two apolar solvents with same dielectric constant but different molecular structure, cyclohexane and dodecane. Whereas both solutions correspond to the well-entangled tube phase, their LVE spectra are quantitatively very different, after correcting for differences in solvent viscosity and density. This is done in order to remove the difference of solvent viscosity or density at different pressure and/or temperature. In this way, the LVE spectra reflect the role of the EHUT self-assembly on the viscoelasticity of the investigated solutions. The most striking difference is the significantly lower plateau modulus in cyclohexane, while the ratio of high-to-low frequencies marking the moduli crossover (intermediate frequency regime of Figure 5) is not altered substantially. This observation is in agreement with literature data showing a clear dependence of the plateau modulus on the number of carbons in the main backbone of the alkane solvent.[62] These results support the hypothesis that the packing of the EHUT molecules depends on the exact bulk properties of the solvent. They refer to the dimensions of solvent molecules, each residing within an effective

parallelepiped with length (*L*), width (*W*) and thickness (*Th*), such that $L \geq W \geq Th$.[33] This rationalizes the fact that the tubes to filaments structural transition takes place at lower temperatures in more bulky aromatic solvents compared to linear alkanes. Increased bulkiness of the solvents leads to destabilization of tube phase. Similarly, comparing the relative viscosities of the solutions in different solvents, lower viscosities are observed in aromatic solvents compared to linear alkanes (like dodecane), which implies changes in the length of the assemblies. Given that the phase diagrams in EHUT are quantitatively (but not qualitatively) different, we include on the same figure the LVE data for the EHUT/dodecane solution at 65°C, which corresponds to almost the same distance from the tube-to-filament transition temperature as the EHUT/cyclohexane solution at 25°C. We can now compare this spectrum with that in cyclohexane at 25°C: there remains a (smaller) difference in the plateau moduli, however the extend of the intermediate frequency regime differs by nearly a decade. Hence, clearly the solvent's molecular structure plays a key role on the dynamics of the supramolecular polymer solutions. The solid lines through the data in the terminal regime are fits with the Maxwell model which normally works well in simple wormlike surfactant micelles. The fits nicely capture the terminal times (see also Ref.38) but the experimental plateau region is more complicated (not clear plateau but rather a weakly frequency-dependent regime) for these hydrogen-bonded semiflexible supramolecular tubes. See also discussion on Cole-Cole representation and semiflexible chain modeling below.

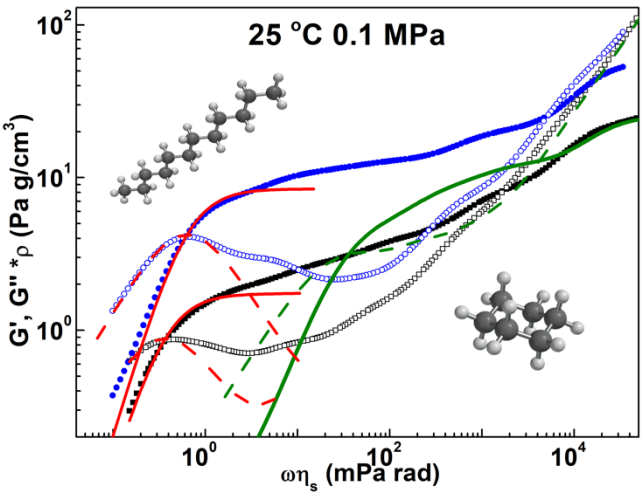

Figure 6: Linear viscoelastic spectra (filled symbols or full line for G', open symbols or dashed line for G'') of EHUT solutions in dodecane (3.6 g/L, blue circles) and cyclohexane (4 g/L, black squares) at 0.1 MPa and 25°C. Data for EHUT/dodecane (3.6 g/L, 65 °C) corresponding to the same distance from the tube-to-filament transition temperature as the EHUT/cyclohexane solution at 25°C, are also shown (green

lines). The moduli are scaled with solvent density and the frequency with solvent viscosity. The cartoons show the molecular structures of dodecane (top) and cyclohexane. The solid and dashed red lines are Maxwell model fits of G' and G'' respectively, yielding G_p=8.3Pa, =1.6s (for dodecane solutions) and G_p=1.7Pa, =2.6s (for cyclohexane solutions).

RESULTS AND DISCUSSION

The phase diagram of EHUT solutions in toluene has been investigated extensively at atmospheric pressure.[34] As shown in Figure 1, depending on concentration and temperature, EHUT solutions may be monomeric (unassembled) or form long self-assembled thin filaments or tubes. Tube structures have a persistence length of at least 100 nm, as extracted from neutron scattering measurements (filaments are much shorter and accurate estimation of their persistence length through scattering techniques was extremely difficult).[40] Toluene is slightly less apolar compared to dodecane and cyclohexane (its dielectric constant is 2.38).[54] In dodecane, which is of worst quality for the polar parts of EHUT, the tube structure is stabilized as opposed to toluene, and consequently, some qualitative differences in dynamics exist.[35, 64] Recently, we combined bulk and passive microrheology to perform a systematic characterization of the phase diagram of EHUT/dodecane at ambient pressure.[65] The transition between tubes and filaments was found to take place at about 88°C in the semidilute regime. Dodecane has been a popular choice for conventional rheological measurements, in part because of its high boiling point at atmospheric pressure (which minimizes the risk of evaporation). The effects of pressure will be discussed below.

Pressure-induced transition from unentangled (UE) to well entangled (WE) assemblies

Figure 7 depicts characteristic LVE spectra for EHUT/dodecane (7a) and EHUT/cyclohexane (7b) at different pressures. Additional data (more pressures) are presented in Figure S3. The temperature and concentration were chosen so that at ambient pressure EHUT self-assembles into short unentangled (UE) tubes and UE filaments in dodecane and cyclohexane, respectively. The evolution of the LVE spectra with pressure and their qualitative and quantitative differences are evident. We attribute the changes of the LVE spectra to significant changes in the average length of the assemblies. The shapes of the spectra are so different because by increasing the pressure there is a change in <L> and transition from unentangled to partially (weakly) entangled to well entangled regimes.[65] The well entangled regime exhibits an extended plateau region whereas the partially entangled is characterized by a weak viscoelastic regime ; the latter

has a weak plateau that decays faster with decreasing frequency than that of the well entangled regime. Nonetheless, the partially entangled regime remains clearly different from the Zimm-like untentangled regime which has well separated moduli with G''>G'.[65] An alternative representation of the LVE spectra in terms of the so-called Cole-Cole plot is discussed below.

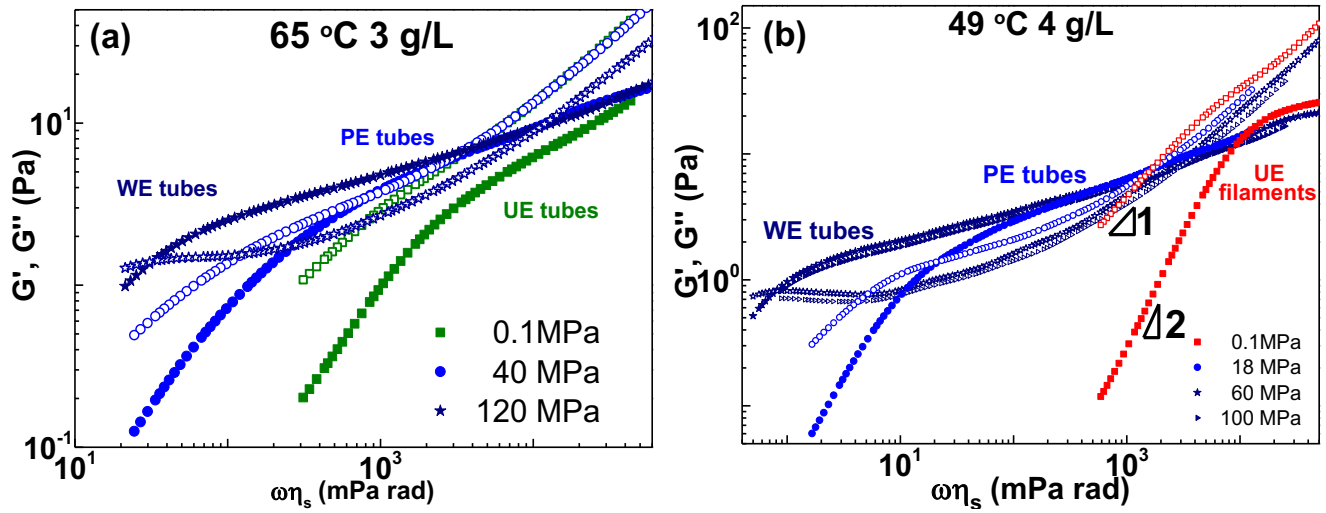

Figure 7: Microrheological storage and loss moduli (G' and G'', respectively) as a function of frequency (scaled with the solvent viscosity) for (a) EHUT/dodecane at c=3 g/L and T=65°C, and (b) EHUT/cyclohexane at c=4 g/L and T=49 °C and different pressures (indicated in the legend). G' data are represented by filled symbols and G'' data by open symbols. Terminal slopes are indicated (1,2), while the state of the different solutions (UE, PE, WE) is also indicated (see text).

Concerning the latter, Figure 8 shows the pressure dependence of the ratio between the HF and LF moduli crossover frequencies (arrows in Figure S3),$w_e = \frac{\omega_{HF}}{\omega_{LF}}$, which actually represents the extend of the intermediate frequency regime. In this context, Figure S4a reports the concentration dependence of w_e at 0.1 MPa and 100 MPa. The large values (w_e >300) of this ratio at high pressures are consistent with the well-entangled regime (see also Figures 10 and 11 below) and with data in the literature.[53,65] The pressure dependencies of the fast and terminal times at 1 g/L EHUT/ dodecane solution are presented in Figure S4b (see also Figure S5). Note that, as already mentioned, the measurements were performed at conditions of ambient humidity, corresponding to a relative value of about RH=43%. Although examining the role of humidity is beyond the scope of this investigation, we have nevertheless examined the influence of humidity by saturating the atmosphere with water vapor (reaching RH≈93%) and observed the time needed to reach ambient conditions (steady state), which is actually long (Figure S6). We therefore consider that we have steady-state conditions at ambient humidity.

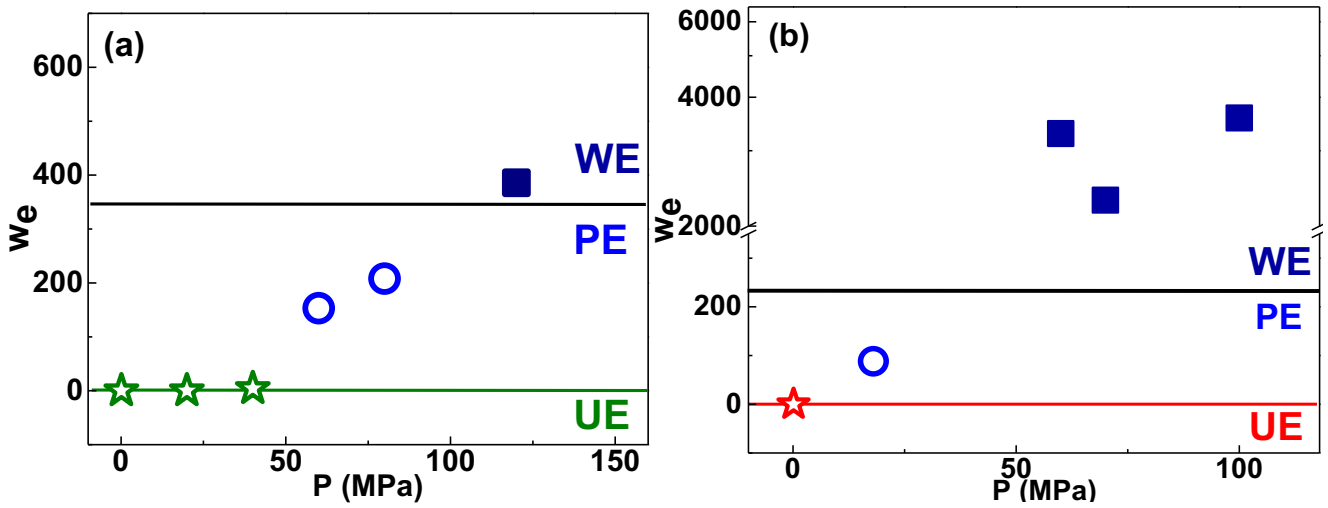

Figure 8: Ratio of high- to low-frequency moduli crossover (w_e) as a function of pressure for (a) EHUT/dodecane solution (c = 3 g/L) and (b) EHUT/ cyclohexane solution (c = 4 g/L). Lines separate the three different regimes: UE (open red stars), PE (open blue circles) and WE (filled blue squares).

The relative viscosity increment ($\eta_i = \frac{\eta_0^*}{\eta_s} - 1$) can be extracted from the LVE data, and its pressure dependence for different temperatures and concentrations is depicted in Figure 9 at elevated pressures for EHUT/dodecane (9a) and EHUT/cyclohexane (9b) solutions. This representation suggests that, for both solutions at constant pressure, an increase of temperature will reduce the relative viscosity increment, consistently with the change of LVE spectra of Figure 7 and in agreement with our recent work.[65] More importantly, there is a weak increase of η_i with pressure up to about 60 MPa, which is attributed to a change of the average length <L> of the supramolecular polymers. For P>60 MPa, in the WE regime, η_i becomes essentially independent of pressure.

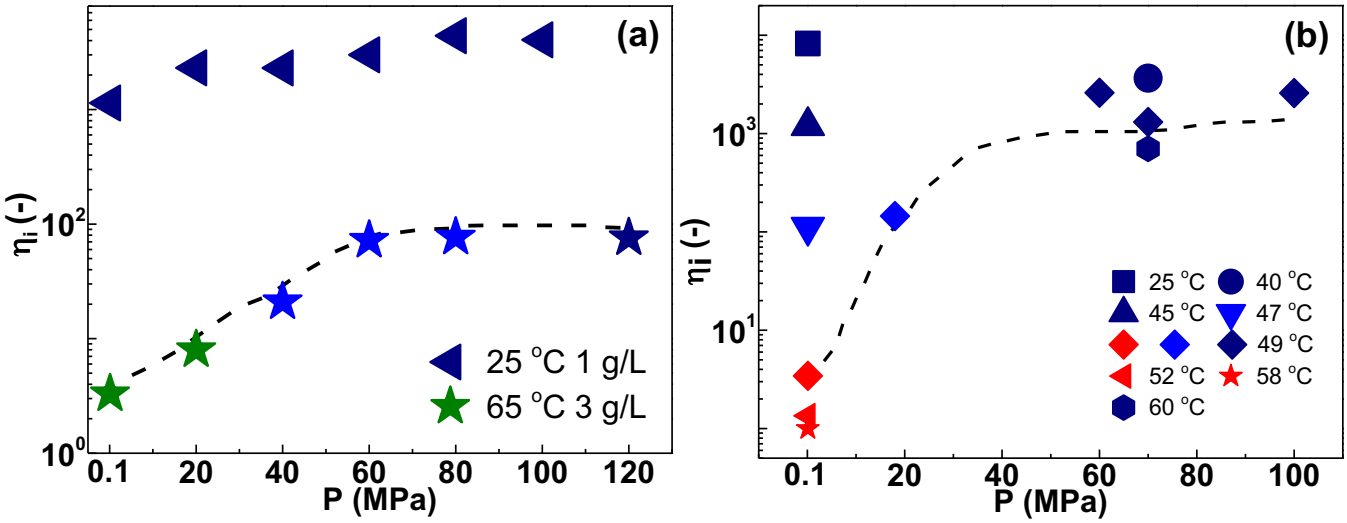

Figure 9: (a) Relative viscosity increment $\eta_i = \eta_0^*/\eta_s$ -1 as a function of pressure for different EHUT /dodecane solutions (concentrations and temperatures are marked on the legend). Green, light blue and dark blue symbols indicate unentangled, partially entangled and well entangled solutions. The dashed lines are drawn to guide the eye. The viscosities of 1 g/L at 25°C are actually obtained from fitting the dynamic viscosity data of Figure S5 with the Carreau model (left-pointing triangles). (b) Respective data for an EHUT /cyclohexane solution at c = 4 g/L and different temperatures indicated on the legend. Red symbols correspond to filaments, the rest to tubes.

Concentration dependence at 0.1 and 100 MPa of WE assemblies

To better appreciate the effects of pressure, we first compare the LVE spectra at 0.1 and 100 MPa for two different concentrations. In Figure 10, the impact of pressure on the solvent background is accounted for by multiplying the frequency with the pressure-dependent solvent viscosity (see also Figure S2). This normalization collapses both the G' and G'' data at high frequencies, especially at the high-frequency crossover and above, as observed for 1.5 g/L (Figure 10a). This regime reflects the small-scale (local) response of the supramolecular polymer at times below the (fast) breaking time (τ_f), which is mediated by the solvent.[14,66, 67] Moreover, the influence of pressure on the terminal relaxation is evident in this figure and appears to relate to a structural change within the well-entangled tube region of the phase diagram, as also corroborated by the more extended and slightly increased plateau modulus at 100 MPa. This structural change should be associated with the length distribution due to the living nature of the self-assembly and the interplay of breaking and terminal times. The latter appears to be more evident at the higher concentration where the minimum in G'' is shifted to lower frequencies by roughly a factor of about 5, a bit smaller than the shift of the terminal crossover frequency (Figure 10b). This structural change should

be related to a pressure-induced state transition (reported below) owing to changes in the average length of the assemblies, <L>.[68-70] Note that concentrations above 5 g/l and low temperatures (below 25°C) were not investigated. In that regime, the solutions become non-ergodic and the use of a multi-speckle DLS setup (with a CCD camera replacing the PMT and a linear correlator) is warranted.[71, 72] This will be the subject of future studies.

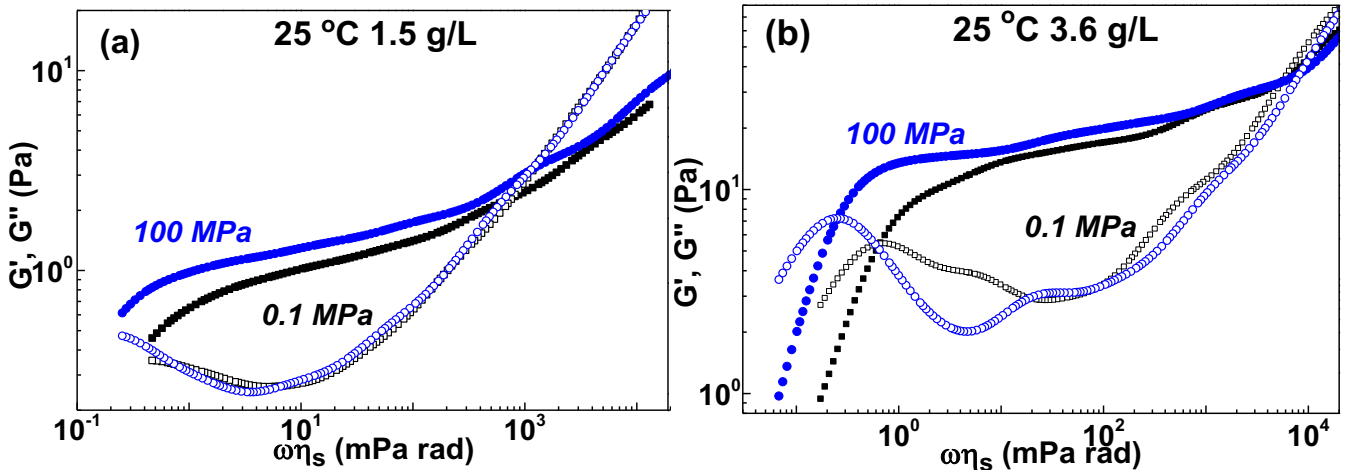

Figure 10: G' (filled symbols), G'' (open symbols) for EHUT/dodecane solutions at T=25°C, as a function of frequency multiplied by solvent viscosity, at 0.1 MPa (black squares) and 100 MPa (blue circles). Data are depicted for two different concentrations, (a) 1.5 g/L and (b) 3.6 g/L. Accounting for the difference in solvent density from 0.1 to 100 MPa (746 to 799 kg/m^3) does not have any appreciably effect on the data.

Figure S7 depicts the C(t) data (S7a,b) and the respective MSD (S7c) results from measurements of EHUT/dodecane solutions (with PMMA probes) at different concentrations, 25°C and pressures of 0.1 MPa (S7a) and 100 MPa (S7b). The effect of high pressure in slowing-down the dynamics is evident across all concentrations (see also the comparison of the unshifted LVE spectra at 0.1 and 100 MPa in Figure S8). More data are depicted in Figure S9 for dodecane and Figure S10 for cyclohexane. We note that, with increasing concentration a second relaxation process emerges, which becomes stronger and dominates the solution's response at higher concentrations (Figures S7a, b). Simple observation of the C(t) data suggests that the pressure affects the slow process more significantly compared to the fast one. Figure 10 shows MSD and LVE data of the same solutions at 25 °C, 100 MPa and different concentrations. For concentrations c≥1 g/L an intermediate plateau is probed in both MSD (10a) and LVE (10b) data, and the sub-diffusive motion inferred from MSD reflects the presence of an entanglement network. In fact, the available data suggest that between 0.75 and 1 g/L the transition from unentangled (UE) to well-entangled

(WE) tubes takes place. At 25°C and low concentration in the unentangled regime (0.75 g/L, Figure S9a) the LVE data exhibit a small difference when the pressure increases from 0.1 to 100 MPa, however no state transition is detected in the examined temperature regime (see also Figures S8 and S9b,c,d). At 3.6 g/L in dodecane, the entire LVE spectrum with the terminal regime (Figures 11b and S8b) and respective time-dependent MSD with terminal diffusive slope (Figure 11a) are well-captured. Moreover, the high-frequency dependence of G'' appears to conform to a power-law with exponent of about 0.75, as reported for other living and semiflexible polymers.[14,46, 47, 68-70] Whereas this is an interesting finding and seems to be robust, we note the data should be considered with caution because they are extracted from the original C(t) data, as already discussed. We further note that analysis of the entire LVE spectrum of the EHUT solutions in the context of semiflexible chains models[68-70] involves some parameters controlling the three contributions to the modulus (curvature, orientation, tension) which cannot be readily determined. Importantly, the role of the break-reformation time should be considered. At the same time, as we noted above in conjunction with the data of Figure 6, the terminal regime can be described well by a Maxwell mode but there is a slight discrepancy in the plateau modulus. Hence, a rigorous analysis should be made in the context of living polymers models, [45-50] accounting for local stiffness, and this would be the subject of future work.

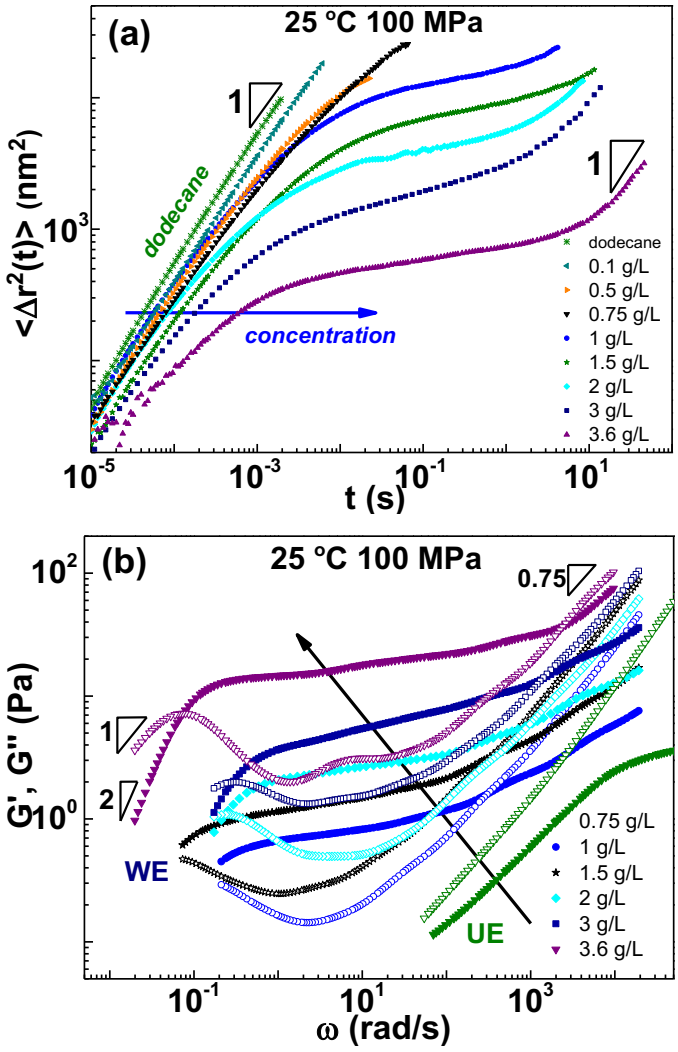

Figure 11: (a) Time-dependent mean square displacement $\langle \Delta r^2(t) \rangle$ of EHUT/dodecane solutions with added PMMA tracer particles (see text) at different EHUT concentrations (indicated in the legend), from 0 (dodecane) to 3.6 g/L, at T = 25 °C and 100 MPa. The diffusive long-time behavior with slope of 1 is indicated. (b) microrheological frequency-dependent linear viscoelastic moduli (storage G': filled symbols; loss G'': open symbols) of the same solutions at fewer concentrations (for clarity). The arrows show the direction of increasing concentration (with changing state from UE to WE). The terminal slopes are also indicated. See also Figures S8, S12.

Based on the above results, we construct a dynamic state diagram for EHUT/dodecane solutions in the temperature-pressure space for concentrations which correspond to the tube phase (analogous to Figure 1 b). This diagram, in Figure 12, shows how changing pressure can lead to different dynamic states of the supramolecular solutions, UE, PE and WE, depending on the concentration and temperature regime (see also Figures 11 and S9 for dodecane, and Figure S10 for cyclohexane). At fixed pressure, increasing

temperature promotes the unentangled state of tubes (and also the tube to filament transition).[14] The different states should reflect a different length distribution of the self-assemblies.[53,65,73]

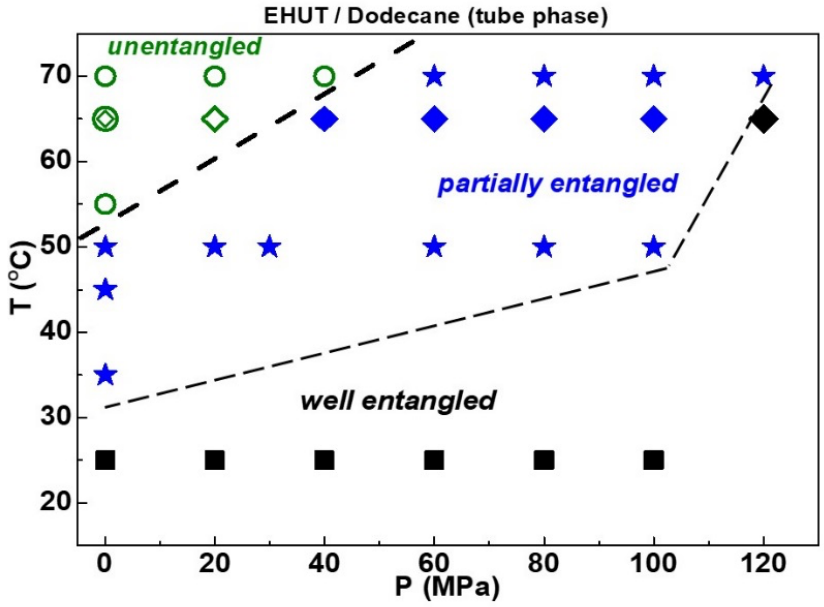

Figure 12: State diagram in terms of temperature versus pressure for EHUT/ dodecane solutions at different concentrations in the tube phase. Green open symbols represent unentangled solutions, blue filled stars partially entangled and black filled squares well-entangled solutions. All data are taken at 1 g/L, except for those represented by filled diamonds which are taken from a 3 g/L EHUT/dodecane solution at 65°C (blue refer to partially entangled and black to well-entangled solutions). At 0.75 g/L and 25 °C we have unentangled tubes in this pressure range. The dashed lines are drawn to guide the eye.

The analysis of the LVE spectra reveals the concentration dependence of different characteristic quantities, which are presented in Figure 13 for different situations. First, we note that the effective plateau modulus G_p is actually the value of G' corresponding to the frequency marking the minimum of G'' in Figure 11b (see also Figure S12) and is virtually unaffected by pressure (Figure 13a) and humidity (also, at atmospheric pressure the microrheology data coincide with data obtained by bulk rheometry).[38] The power-law dependence $G_p \sim c^2$, is consistent with theoretical predictions by Cates.[45-48] The same figure also depicts the evolution of persistence length l_p at 0.1 and 100 MPa, and again there is no appreciable effect of pressure, with a typical size being about 50 nm (in good agreement with literature values for similar systems), extracted from the high frequency marking the moduli crossover (see also Figure S13); we note again that some uncertainty in the microrheological data extracted from the C(t) in this regime cannot be excluded.[14,53,63] Note that information about the LVE properties can be obtained from the Cole-

Cole representation of G'' vs G', which is depicted in Figure S14. It can indeed pinpoint the deviation from Maxwell model (associated with a complete semi-circle of data) is obtained, the minimum of G'' is associated with the persistence length of the supramolecular polymer.[45,65,74,75] However, this was not always the case with the present EHUT samples. It is nevertheless clear from Figure S14, that on increasing and/or concentration, this supramolecular polymer tends toward a truly Maxwellian behavior. On the other hand, the terminal relaxation time τ_t is affected by pressure at ambient humidity (Figure 13b), as is also affected by humidity at ambient pressure.[38] For both 0.1 and 100 MPa, the data conform to a scaling $\tau_t \sim c^{0.77}$, with the exponent being identical to that reported recently in the literature for reduced humidity conditions.[38] On the other hand, the fast relaxation time τ_f becomes slower at high pressures (reflecting the increase of solvent viscosity with pressure, as already discussed above) and speeds-up with concentration above 5 g/L, exhibiting the same scaling $\tau_f \sim c^{-2}$ for 0.1 and 100 MPa (Figure 13c, gray-shaded region). The analysis of the C(t) data (fast modes in Figures S7, S11) yields the characteristic correlation length (hydrodynamic mesh size, ξ_H) of EHUT/dodecane solutions, which is plotted as a function of concentration for different pressures in Figure 13d. Increasing pressure reduces ξ_H (see also Figure S11b), and for concentrations exceeding 1.5g/L all data appear to conform to the $\xi_H \sim c^{-0.75}$ scaling for flexible chains in the semidilute regime (gray-shaded region in Fig.13d).[76] Respective data of EHUT/cyclohexane solutions are also included in the plot of Figure 13d. We note again that DLS-microrheology measurements were performed at different levels of humidity (Figure S6), and the basic result of humidity-induced speed-up of dynamics was confirmed.[38]

In summary, the above results show that pressure is an important control parameter in the design and manipulation of supramolecular polymers. Increasing pressure slows-down both the fast and terminal dynamics, but its effects are not equivalent to those of inverse temperature. We believe that pressure affects the interplay of breaking and recombination of hydrogen bonds and this seems to be the underlying factor for the changes in dynamics (as well as statics). Undoubtedly, molecular simulations are warranted here to elucidate the details of the coupling of high pressure and hydrogen bonding, including stability and directionality, as shown recently with small associating molecular species.[77,78]

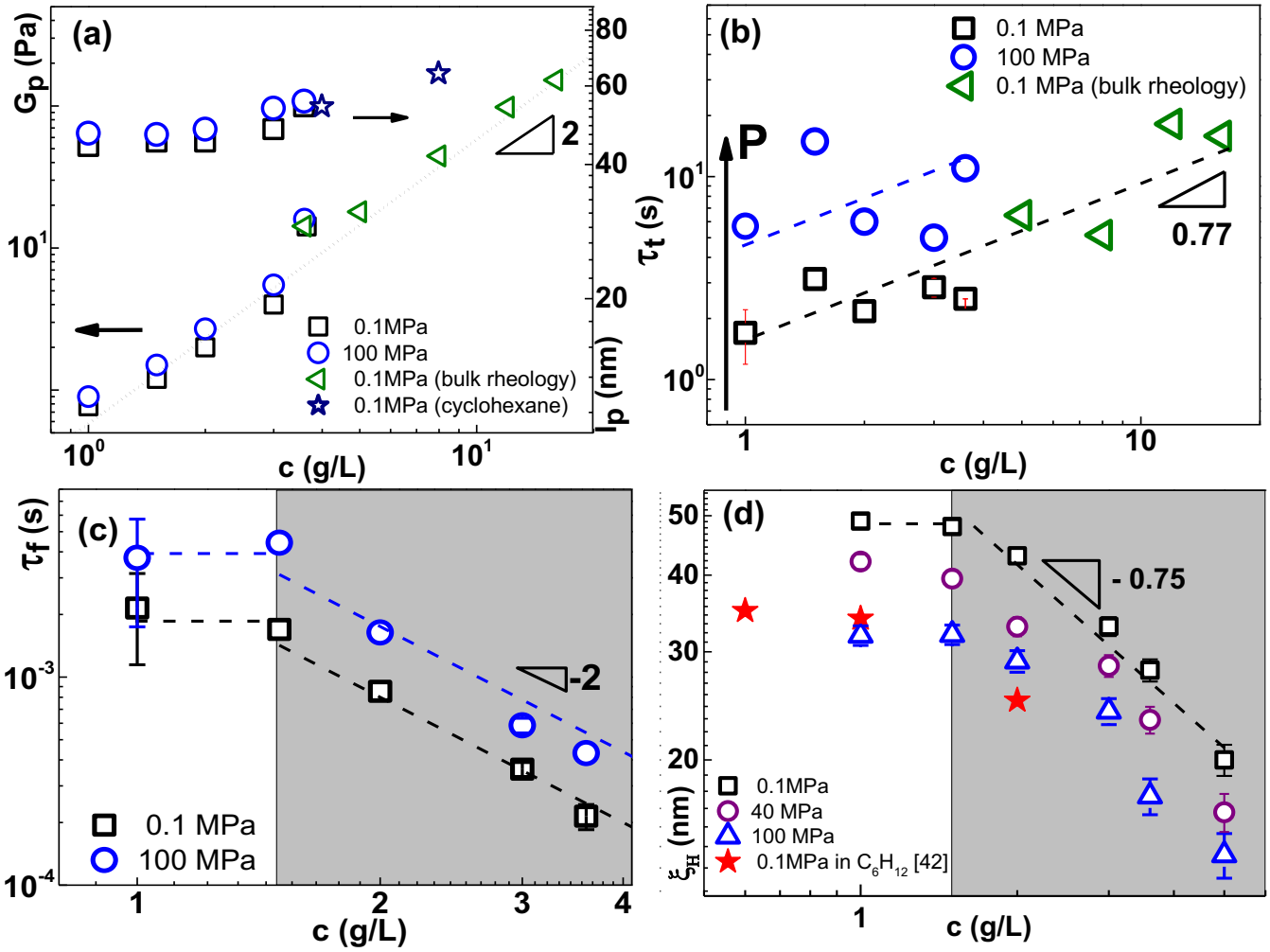

Figure 13: (a) Experimental plateau modulus Gp versus concentration c, at T=25 ^{O}C for EHUT in dodecane, extracted from microrheology (0.1 MPa: squares; 100 MPa: circles) and bulk rheology (0.1 MPa: left-pointing triangles). Also plotted as the respective persistence length data (lp) (right vertical axis). The star symbols refer to lp data of EHUT/cyclohexane solutions at ambient pressure.[14] (b) Respective terminal relaxation time τ_t versus concentration c, extracted from bulk rheology at 0.1 MPa (open triangles) and microrheology at different pressures (open squares at 0.1 MPa, open circles at 100 MPa). (c) Fast relaxation time τ_f extracted from the high-frequency moduli crossover, as a function of concentration at 0.1 MPa (squares) and 100 MPa (circles); the gray-shaded region indicates the decrease with power-law of -2. (d) Hydrodynamic mesh size, ξ_H as a function of concentration c, for solutions in dodecane at different pressures (see legend) and in cyclohexane at ambient pressure (red star symbols) (see also Figure S13); the gray-shaded region indicates the decrease with power-law of -0.75. Lines have sloped indicated on the plots.

IV. CONCLUSIONS

High-pressure passive microrheology is emerging as an efficient, robust technique for determining the linear viscoelastic properties of soft materials and represents an important complement to the existing rheometric techniques. In this work, we have presented a robust methodology to investigate the dynamics and linear viscoelastic properties of supramolecular polymers at elevated pressures up to 120 MPa. To this end, we have employed dynamic light scattering in the single scattering limit which allows obtaining the intermediate scattering function at different scattering angles (here we have used only one), temperatures and pressures. The linear viscoelastic spectrum over a wide range of frequencies was presented for the 2,4-bis (2-ethylhexylureido)toluene (EHUT) hydrogen-bonding motif, which forms supramolecular polymers in two apolar solvents, n-dodecane and cyclohexane. Our findings indicate that, depending on the solvent, pressure may have a huge impact on the phase behavior of the supramolecular assemblies and in particular promote the entangled tube (wormlike micellar) phases (partially entangled and, eventually, well entangled). Increasing pressure (in the range 0.1 to 60 MPa) is found to affect the hydrodynamic correlation length ξ_H and the relaxation times τ_f and τ_t more than the plateau modulus G_p or the persistence length l_p (which are practically unaffected), and this is attributed to changes of the length distribution of the self-assemblies. Over a small concentration range, G_p, ξ_H, τ_f and τ_t exbibit power-law dependencies on concentration with exponents 2, -0.75, -2 and 0.77, respectively (for l_p there is no unambiguous evidence of appreciable concentration dependence), practically for all pressures. A temperature-pressure state diagram has been constructed from the experimental data of the EHUT/dodecane solutions at different concentrations (in the tube regime), demonstrating the pressure-induced unentanged-to-entangled and temperature-induced well entangled to partially entangled to unentangled transitions, respectively.

SUPPORTING INFORMATION

DLS passive microrheology data at different times and cycles ; Solvent data ; Extracted LVE microrheology data and analysis ; Effects of humidity, time ; DLS and LVE microrheology data in dodecane ; LVE microrheology data in cychohexane ; DLS data and extracted hydrodynamic mesh sizes; Bulk rheometric LVE data in dodecane ; Extracted parameters (modulus, persistence length) from LVE data; Cole-Cole representation of LVE data.

ACKNOWLEDGMENTS

It is an honour and pleasure to contribute to this special issue of JPC celebrating the science of Professor Doros Theodorou on the occasion of his 65th birthday. Doros' pioneering work on a broad range of topics

associated with physical chemistry and properties of materials, his scholarship and his unfailing enthusiasm for scientific discovery have been a constant source of inspiration to many generations of students and colleagues. We wish him many more years of scientific and moral leadership! We are grateful to A. Larsen and A. Mavromanolakis for technical assistance. Partial support has been received by the European Commission (Horizon2020-INFRAIA-2016-1, EUSMI grant no. 731019) and the Greek Secretariat for Research and Technology (INNOVATION program-AENAO).

REFERENCES

1. Münstedt H. Influence of hydrostatic pressure on rheological properties of polymer melts—A review. *J. Rheol.,* **2020**, 64, 751-774.

2. Ahuja A.; Lee R.; and Joshi Y. M. Advances and challenges in the high-pressure rheology of complex fluids. *Adv. Colloid Interface Sci.*, **2021**, 294, 102472.

3. Boza F. J. M.; and Gallegos C. High Pressure Rheology, in *Encyclopedia of Life Support Systems (EOLSS)*, Developed under the Auspices of the UNESCO, Eolss Publishers, Paris, **2010**.

4. Kulisiewicz L.; Delgado A. High-pressure rheological measurement methods: a review. *Appl Rheol*., **2010**, 20, 13018.

5. Hodge W. A.; Fijan R. S.; Carlson K. L.; Burgess R. G.; Harris W. H.; and Mann R. W. Contact pressures in the human hip joint measured in vivo. *Proc. Natl. Acad. Sci.*, **1986**, 83, 2879–2883.

6. Brooks N.J. Pressure effects on lipids and bio-membrane assemblies. *IUCrJ*, **2014**, 1, 470 —477.

7. Kazarian S.G.; Chan, K.L.A. FTIR Imaging of Polymeric Materials under High-Pressure Carbon Dioxide. *Macromolecules*, **2004**, 37**,** 579-584.

8. Vavrin R.; Kohlbrecher J.; Wilk A.; Ratajczyk M.; Lettinga M.P.; Buitenhuis J. ; Meier G. Structure and phase diagram of an adhesive colloidal dispersion under high pressure: A small angle neutron scattering, diffusing wave spectroscopy, and light scattering study. *J. Chem. Phys*. **2009**, 130, 154903.

9. Patkowski A.; Paluch M.; Kriegs H. Dynamic light scattering studies of supercooled phenylphthalein–dimethylether dynamics under high pressure*. J. Chem. Phys.* **2002***,* 117, 2192-2198.

10. Santos J.J.L.; Martin B.S.; Gasser U.; Nieves A.F. The effect of hydrostatic pressure over the swelling of microgel particles. *Soft Matter*, **2011**, **7**, 6370.

11. Niebuur B. J.; Lohstroh W.; Appavou M. S.; Schulte A.; Papadakis C. M. Water Dynamics in a Concentrated Poly(N-isopropylacrylamide) Solution at Variable Pressure. *Macromolecules.*, **2019**, 52, 1942–1954.

12. Behzadfar E.; Hatzikiriakos S.G. Rheology of bitumen: effect of temperature, pressure, CO_2 concentration and shear rate. *Fuel* **2014**, 116, 578–87.

13. Schmidt J. R.; Wolf B. A. Pressure Dependence of Intrinsic Viscosities and Huggins Constants for Polystyrene in tert-Butyl Acetate. *Macromolecules.* **1982**, 15, 1192-1195.

14. Burger N.A.; Mavromanolakis A.; Meier G.; Brocorens P.; Lazzaroni R.; Bouteiller L.; Loppinet B.; Vlassopoulos D. Stabilization of supramolecular polymer phase at high pressures. *ACS Macro Let*. **2021**, 10, 321–326.

15. Maxwell B.; Jung A. Hydrostatic pressure effect on polymer melt viscosity. *Mod. Plast*. **1957**, 35,174–182.

16. Hatzikiriakos S.G.; Dealy J.M. Role of slip and fracture in the oscillating flow of hdpe in a capillary. *J Rheol.* **1992**, 36, 845-884.

17. Tang H.S.; Kalyon D.M. Unsteady circular tube flow of compressible liquids subject to pressure-dependent wall slip. *J Rheol*, **2008,** 25, 507-525.

18. Cardinaels R.; Van Puyvelde P.; Moldenaers P. Evaluation and comparison of routes to obtain pressure coefficients from high-pressure capillary rheometry data. *Rheol. Acta,* **2007**, 46, 495-505.

19. Hou Y. Y.; Kassim H. O. Instrument techniques for rheometry. *Rev. Sci. Instrum.* **2005**, 76, 101101.

20. Appel E. A.; Biedermann, F.; Hoogland D.; del Barrio J.; Driscoll, M. D.; Hay S.; Wales D. J.; Scherman O. A. Decoupled Associative and Dissociative Processes in Strong yet Highly Dynamic Host−Guest Complexes. *J. Am. Chem. Soc*. **2017**, 139, 12985-12993.

21. Kloxin C. J.; van Zanten J. H. High-pressure phase diagram of an aqueous PEO-PPO-PEO triblock copolymer system via probe diffusion measurements. *Macromolecules*, **2010**, 43, 2084-2087.

22. Tanner S. A.; Amin S.; Kloxin C. J.; Van Zanten J. H. Microviscoelasticity of Soft Repulsive Sphere Dispersions: Tracer Particle Microrheology of Triblock Copolymer Micellar Liquids and Soft Crystals. *J. Chem. Phys.* **2011**, 134, 174903.

23. Dennis K.; Gao Y.; Phathak A.; Sullivan P. F.; Furst E. M. Design, operation, and validation of a microrheology instrument for high-pressure linear viscoelasticity measurements *J. Rheol*. **2020**, 64, 205-212.

24. Weigh T.A. Advances in the microrheology of complex fluids. *Rep. Prog. Phys.* **2016,** 79, 074601.

25. Wojnarowska Z., Rams-Baron M.; Knapik-Kowalczuk J.; Połatyńska A.; Pochylski M.; Gapinski J.; Patkowski A.; Wlodarczyk P. ; Paluch M. Experimental evidence of high-pressure decoupling between charge transport and structural dynamics in a protic ionic glassformer. *Sci. Rep*. **2017**, 7, 7084.
26. Annighöfer B.; Hélary A.; Brûlet A.; Colas de la Noue A.; Loupiac C.; Combet S. A high pressure cell using metallic windows to investigate the structure of molecular solutions up to 600 MPa by small-angle neutron scattering. *Rev. Sci. Instrum*. **2019**, 90, 025106.
27. Kohlbrecher J.; Bollhalder A.; Vavrin R.; Meier G. A high pressure cell for small angle neutron scattering up to 500MPa in combination with light scattering to investigate liquid samples *Rev. Sci. Instr.* **2007**, 78, 125101.
28. Meier G.; Kriegs H. A high pressure cell for dynamic light scattering up to 2kbars with conservation of plane of polarization *Rev. Sci. Instr.* **2008**, 79, 013102.
29. Meier G.; Vavrin R.; Kohlbrecher J.; Buitenhuis J.; Lettinga M. P.; Ratajczyk M. Structure and phase diagram of an adhesive colloidal dispersion under high pressure: A small angle neutron scattering, diffusing wave spectroscopy, and light scattering study. *Mater. Sci. Technol*. **2008**, 19, 034017.
30. Van der Gucht J.; Besseling N.; Knoben W.; Bouteiller L.; Stuart M. C. Brownian particles in supramolecular polymer solutions. *Phys. Rev. E*, **2003**, 67, 051106.
31. Fernandez-Castanon J.; Bianchi S.; Saglimbeni F.; Di Leonardo R.; Sciortino F. Microrheology of DNA hydrogel gelling and melting on cooling. *Soft Matter*, **2018**, 14, 6431-6438.
32. Simic V. Bouteiller L.; Jalabert M. Highly cooperative formation of bis-urea based supramolecular polymers. *J. Am. Chem. Soc*. **2003**, 125, 13148-13154.
33. Pinault T.: Isare B.; Bouteiller L. Solvents with similar bulk properties induce distinct supramolecular architectures. ChemPhysChem. **2006**, **7**, 816-819.
34. Bouteiller L.; Colombani, O.; Lortie F.; Terech, P. Thickness transition of a rigid supramolecular polymer. *J. Am. Chem. Soc.* ***2005***, 127, 8893–8898.
35. Ducouret G.; Chassenieux C.; Martins S.; Lequeux F.; Bouteiller L. Rheological characterisation of bis-urea based viscoelastic solutions in an apolar solvent. *J. Col. & Inter. Sci.* **2007**, 310, 624-629.
36. Lortie F.; Boileau S.; Bouteiller L.; Chassenieux C.; Demé B.; Ducouret G.; Jalabert M.; Lauprêtre M.; Terech P. Structural and rheological study of a bis-urea based reversible polymer in an apolar solvent, *Langmuir*. **2002**, 18, 7218-7222.
37. Bellot M.; Bouteiller L. Thermodynamic description of bis-urea self-assembly: competition between two supramolecular polymers. *Langmuir*, **2008**, 24, 14176-14182.

38. Louhichi A.; Jacob A.R.; Boutteiller L.; Vlassopoulos D. Humidity affects the viscoelastic properties of supramolecular living polymers. *J. Rheol*. **2017**, 61, 1173-1182.

39. Van Zee N. J.; Adelizzi B.; Mabesoone M. F. J.; Meng X.; Aloi A.; Zha R. H.; Lutz M.; Filot I. A. W.; Palmans A. R. A.; Meijer E. W. Potential enthalpic energy of water in oils exploited to control supramolecular structure. *Nature.* **2018**, 558, 100-103.

40. Francisco K. R.; Dreiss C. A.; Bouteiller L.; Sabadini E. Tuning the Viscoelastic Properties of Bis (urea)-Based Supramolecular Polymer Solutions by Adding Cosolutes. *Langmuir.* **2012**, 28, 14531-14539.

41. Lortie F.; Boileau S.; Bouteiller L.; Chassenieux C.; Laupretre F. Chain Stopper-Assisted Characterization of Supramolecular Polymers. *Macromolecules*. **2005**, 38, 5283-5287.

42. Knoben W.; Besseling N.A.M.; Stuart M.A.C. Rheology of a reversible supramolecular polymer studied by comparison of the effects of temperature and chain stoppers. *J. Chem. Phys.* **2007**, 126, 024907.

43. Knoben W.; Besseling N.A.M.; Bouteiller L.; Stuart M.A.C. Dynamics of reversible supramolecular polymers: Independent determination of the dependence of linear viscoelasticity on concentration and chain length by using chain stoppers. *Phys. Chem. Chem. Phys,* **2005**. 7, 2390–2398.

44. Knoben W.; Besseling, N.A.M.; Cohen Stuart, M.A. Chain Stoppers in Reversible Supramolecular Polymer Solutions Studied by Static and Dynamic Light Scattering and Osmometry. *Macromolecules*, **2006**, 39, 2643-2653.

45. Cates M. Reptation of living polymers: dynamics of entangled polymers in the presence of reversible chain-scission reactions. *Macromolecules*, **1987**, 20, 2289-2296.

46. Cates M.; Candau S. Statics and dynamics of worm-like surfactant micelles. *J. Phys.: Cond.Mat.* **1990**, 2, 6869.

47. Cates M.E.; Fielding S.M. Rheology of giant micelles. *Adv. Phys*. **2006**, 55, 799-879.

48. Cates, M. Dynamics of living polymers and flexible surfactant micelles: scaling laws for dilution. *Journal de Physique*. **1988**, 49, 1593-1600.

49. Peterson J.D.; Cates M.E. A full-chain tube-based constitutive model for living linear polymers, *J. Rheol.* **2020**, 64, 1465.

50. Lequeux, F. Structure and rheology of wormlike micelles. *Cur. Op. Col. & Int. Sci.* **1996,** 1, 341-344.

51. Tan, G.; Zou W.; Weaver M.; Larson R. G. Determining threadlike micelle lengths from rheometry. *J. Rheol.,* **2020**, 65, 59-71.

52. Zou W.; Larson R.G. A mesoscopic simulation method for predicting the rheology of semi-dilute wormlike micellar solutions. J. *Rheol.* **2013**, 58, 681-721.

53. Zou, W.; Tan, G.; Jiang, H.; Vogt, K.; Weaver, M.; Koenig, P.; Beaucage, .G.; Larson, R. G. From well-entangled to partially-entangled wormlike micelles. *Soft Matter*. **2019**, 15, 642-655.

54. Solvents and Solvent Effects in Organic Chemistry, Wiley-VCH Publishers, 3rd ed., N.Y. **2003**.

55. Royall, C. P.; Poon W. C. K.; Weeks E. R. In search of hard spheres. *Soft Matter.* **2013**, 9, 17-27.

56. Furst E. M.; Squires T. M. *Microrheology*, Oxford University Press, NY **2017**.

57. Ferrell R. T.; Himmelblau, D. M. Diffusion Coefficients of Nitrogen and Oxygen in Water. *J. Chem. Eng. Data.* **1967***,* 12, 111–115.

58. Caudwell D.R.; Trusler M.; Wakeham W. A. The Viscosity and Density of n-Dodecane and n Octadecane at Pressures up to 200 MPa and Temperatures up to 473 K. *Int. J. Thermophys*. **2004**, 25, 1339-1352.

59. Squires T. M.; Mason T. G. Fluid Mechanics of Microrheology. *Ann. Rev. Fl. Mech.* **2010**, 42, 413-438.

60. Weese J. A regularization method for nonlinear ill-posed problems. *Comp. Phys. Com.,* **1993**, **77**,429-440.

61. Mason T. G. Estimating the viscoelastic moduli of complex fluids using the generalized Stokes-Einstein equation*. Rheol. Acta.* **2000**, *39*, 371-378.

62. Alvarenga B. G.; Raynal M.; Bouteiller L.; Sabadini E. Unexpected Solvent Influence on the Rheology of Supramolecular Polymers. *Macromolecules* **2017**, 50, 6631-6636.

63. Willenbacher, N.; Oelschlaeger, C. ; Schopferer, M. ; Fischer, P.; Cardinaux, F.; Scheffold, F. **Broad Bandwidth Optical and Mechanical Rheometry ofWormlike Micelle Solutions.** ***Phys. Rev. Lett.*** **2007, *99*, 068302.**

64. Isare B.; Pensec S.; Raynal M.; Bouteiller L. Bisurea-based supramolecular polymers: From structure to properties. *Comptes Rendus Chim*. **2016**, 19, 148–156.

65. Burger N.A;, Pembouong G.; Bouteiller L.; Vlassopoulos D.; Loppinet B. Complete dynamic phase diagram of a supramolecular polymer. *Macromolecules* **2022**, 55, 2609–2614.

66. Athanasiou T. Auernhammer G.K.; Vlassopoulos D.; Petekidis G. High-frequency rheometry: validation of the loss angle measuring loop and application to polymer melts and colloidal glasses. *Rheol. Acta.* **2019**, 58, 619-637.

67. Schroyen, B.; Vlassopoulos, D.; Van Puyvelde P.; Vermant J. Bulk rheometry at high frequencies: a review of experimental approaches. *Rheol. Acta* 2020*,* 59, 1-22.
68. Morse, D. C. Viscoelasticity of Tightly Entangled Solutions of Semiflexible Polymers. 1. Model and Stress Tensor. *Macromolecules,* **1998**, 31, 7030–7043.

69. Morse, D. C. Viscoelasticity of Concentrated Isotropic Solutions of Semiflexible Polmers. 2. Linear Response. *Macromolecules,* **1998**, 31, 7044–7067.

70. Morse, D. C. Viscoelasticity of Tightly Entangled Solutions of Semiflexible Polymers. *Phys. Rev. E* **1998**, 58, R1237–R1240.

71. Kirsch, S.; Frenz, V.; Schärtl, W.; Bartsch, E.; Sillescu, H. Multispeckle Autocorrelation Spectroscopy and Its Application to the Investigation of Ultraslow Dynamical Processes. *J. Chem. Phys.* **1996**, 104, 1758−1761.
72. Duri, A.; Bissig, H.; Trappe, V.; Cipelletti, L. Time-Resolved-Correlation Measurements of Temporally Heterogeneous Dynamics, *Phys. Rev. E*. **2005**, 72, 51401.
73. Massiera G.; Ramos L.; Ligoure C. Role of the size distribution in the elasticity of entangled living polymer solution. *Europhys. Lett.* **2002**, 57, 127-133.
74. Granek R , Cates M.E . Stress relaxation in living polymers: results from a Poisson renewal model. *J. Chem. Phys.*, **1992**, 96, 4758–67.

75. Vereroudakis E.; Vlassopoulos D. Tunable dynamic properties of hydrogen-bonded supramolecular assemblies in solution. *Prog. Polym. Sci*., **2021**, 112, 101321.

76. De Gennes, P. G. *Scaling Concepts in Polymer Physics*. Cornell University Press: Ithaca, NY, **1979**.

77. Fanetti, S.; Citroni, M.; Dziubek, K.; Medre Nobrega, M.; Bini, R. The role of H-bond in the high-pressure chemistry of model molecules. *J. Phys.: Condens. Matter* **2018**, 30, 094001.

78. Clarke S. M.; Steele B. A.; Kroonblawd M. P.; Zhang, D.; Kuo I.-F. W.; Stavrou, E. An isosymmetric high-pressure phase transition in α-glycylglycine: a combined experimental and theoretical study. *J. Phys. Chem*. *B.* **2020**, 124, 1-10.